

Pattern Evolution Caused by Dynamic Coupling between Wetting and Phase Separation in Binary Liquid Mixture Containing Glass Particles

Hajime Tanaka

Institute of Industrial Science, University of Tokyo, Minato-ku, Tokyo 106, Japan

Andrew J. Lovinger and Don D. Davis

AT&T Bell Laboratories, Murray Hill, New Jersey 07974

(Received 27 May 1993)

We demonstrate here that the pattern evolution in a binary liquid mixture containing glass spheres is strongly affected by the dynamic coupling between phase separation and wetting. Because of the difference in the wettability to glass between the two phases, the glass particles are preferentially included in the more wettable phase. The resulting pattern is strongly dependent on whether the spheres are mobile or immobile. For a high density of mobile particles, we find that an initially random pattern of spheres transforms into an ordered pattern because of geometrical confinement of particles into the more wettable phase.

PACS numbers: 64.75.+g, 05.70.Fh, 61.41.+e, 68.45.Gd

Phase separation has so far been studied as a bulk phenomenon [1]; however, it has recently been revealed that the behavior can be strongly affected by wetting phenomena [2] in metastable or unstable states [3,4]. The dynamic coupling between phase separation and wetting is a new problem, and its study has been initiated only very recently. So far the study of wetting phenomena has been limited to wetting on fixed solid walls including gels [5]. However, if solid walls or particles are movable, their motion could be involved in the pattern-evolution process as a result of the dynamic coupling between wetting and phase separation. Here we consider binary polymer mixtures containing solid particles. As an ideal system, we choose monodisperse glass spheres as solid particles and study the pattern evolution caused by phase separation. The cooperative effect between phase separation and dynamic wetting leads to an interesting pattern evolution in the system. This problem is analogous to the problem of aggregation of colloidal particles in binary mixtures [6]. Here, however, the direct, real-space observation allows a detailed dynamic understanding of the role of wetting on particle ordering. In this Letter, we provide the first experimental study on the pattern evolution in unstable states for polymer mixtures containing microscopic glass particles.

The binary mixture studied was a blend of oligomers of styrene (OS) and ϵ -caprolactone (OCL). The weight-average molecular weights of OS and OCL were 1000 and 2000, respectively. The polydispersity ratios M_w/M_n were 1.05 and 1.2 for OS and OCL, respectively. This mixture has an upper-critical-solution-temperature (UCST) phase diagram, where the critical composition ϕ_c is OCL/OS=3/7 and the critical temperature $T_c = 135.0^\circ\text{C}$. It is known that OCL is more wettable to glass than OS because of its higher polarity. Two grades of monodisperse spherical glass particles were used: GP1 having a diameter of $3.786 \pm 0.027 \mu\text{m}$, and GP2 with a diameter of $7.088 \pm 0.050 \mu\text{m}$. The polymer mixture was carefully mixed mechanically with the glass parti-

cles to yield a homogeneous, random distribution. After blending, the mixture was sandwiched between two glass plates. The thickness of the sample d was controlled by a spacer. One series of experiments was done without a spacer. In this case the glass spheres also acted as spacers, and most particles were hard to move because of the friction to the glass plates. In the other series of experiments the spacers consisted of the larger size GP2 spheres; in this case, the smaller particles (GP1) used as fillers could freely move inside the two-dimensional sample. It should be noted that the number density of GP2 spheres which act as spacers is always negligibly small (typically the order of 10^2 cm^{-2}), and thus GP2 spheres should not be regarded as a component of the mixture. Namely, the mixture is composed of two monodisperse polymers and a single kind of monodisperse sphere (GP1). Since the ratio in sphere diameters was below a factor of 2, there was no possibility for overlapping of particles within the spacing. We use this special setting simply to avoid the overlapping of sphere images and get an ideal two-dimensional microscopic image [7]. Samples were quenched to the desired temperatures either within a microscope hot stage (Linkam TH-600R) for a shallow quench within 10 K, or (for a deeper quench) by rapidly transferring them from a hot stage (Mettler MP-500) whose temperature was above T_c to a hot stage kept at the final temperature. The pattern-evolution dynamics was studied by using video microscopy. The patterns were quantitatively interpreted through use of a digital image analysis method [8].

Figure 1 shows the pattern evolution observed in the OCL/OS (3/7) mixture containing glass particles (GP1) without spacers (GP2) at 100°C . The number density ρ_n of the GP1 spheres is $\sim 1.2 \times 10^6 \text{ cm}^{-2}$. Their volume loading fraction Φ_{GP} is $\sim 9\%$ and their projected-area loading fraction S_{GP} is $\sim 14\%$. In this case, the more wettable OCL-rich phase forms domains around the glass particles to reduce the solid-liquid interfacial energy. Since the glass spheres are not free to move,

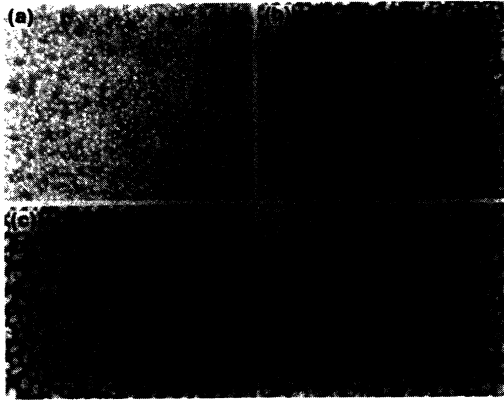


FIG. 1. Pattern evolution in OCL/OS (3/7) containing fixed glass particles at 100°C. (a) 25 s, (b) 60 s, (c) 240 s, and (d) 720 s after the quench. The bar corresponds to 100 μm .

only those glass particles that are close enough can be bridged by the OCL-rich phase. The coarsening process completely stops in this rather early stage, because of the spatial pinning of droplet domains by the fixed glass particles.

Figure 2 shows the pattern evolution observed in the OCL/OS (3/7) mixture containing both glass particles (GP1) and spacers (GP2), at 100°C. Here ρ_n is $2.0 \times 10^6 \text{ cm}^{-2}$ ($\Phi_{\text{GP}} \sim 8.0\%$ and $S_{\text{GP}} \sim 23\%$). In this case, the initial pattern evolution is similar to that of Fig. 1. The more wettable OCL-rich phase forms droplets around the glass particles. However, here the glass particles that are bridged by the OCL-rich phase can now move to reduce the interfacial energy between the two coexisting phases. This mobility of the glass particles causes striking differences in the pattern formation between Figs. 1 and 2, where the glass particles are seen to be segregated into droplets. The droplets containing the glass particles gradually coarsen mainly by wetting-induced interactions between the wetting layers on particles and those on the glass plates.

Figures 3(a)–3(c) show the dependence of the pattern evolution on the volume fraction of the glass particles for the OCL/OS (3/7) mixtures containing both glass particles (GP1) and spacers (GP2). Here ρ_n are $0.8 \times 10^6 \text{ cm}^{-2}$ ($\Phi_{\text{GP}} \sim 3.2\%$ and $S_{\text{GP}} \sim 9\%$) for (a); $\rho_n \sim 1.3 \times 10^6 \text{ cm}^{-2}$ ($\Phi_{\text{GP}} \sim 5.2\%$ and $S_{\text{GP}} \sim 15\%$) for (b); $\rho_n \sim 4.7 \times 10^6 \text{ cm}^{-2}$ ($\Phi_{\text{GP}} \sim 19\%$ and $S_{\text{GP}} \sim 53\%$) for (c). The quench depth and the phase separation time are the same for all three cases; thus ρ_n is the only variable. In all cases, the OCL-rich phase preferentially wets the glass particles. For the low particle density [Fig. 3(a)], a droplet structure is formed, which gradually coarsens with time. For the medium particle density [Fig. 3(b)], an interconnected structure is formed and the pattern also coarsens with time. For the high particle density [Fig. 3(c)], the interconnected pattern is again formed, but in this case the coarsening slows down sig-

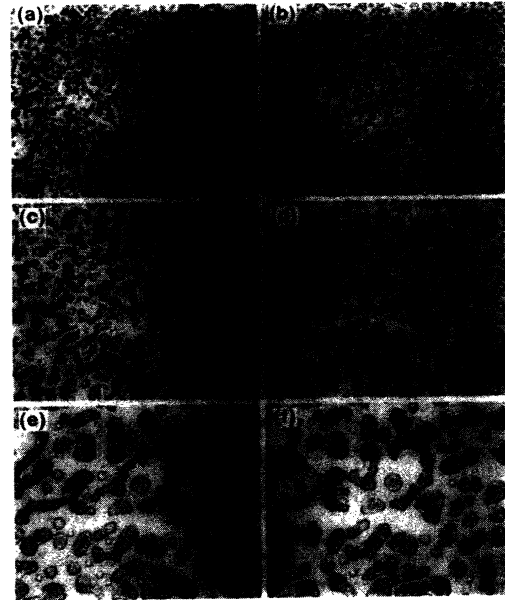


FIG. 2. Pattern evolution in OCL/OS (3/7) containing mobile glass particles at 100°C. (a) 1 s, (b) 2 s, (c) 4 s, (d) 10 s, (e) 110 s, and (f) 950 s after the quench. The bar corresponds to 100 μm .

nificantly because the glass spheres assemble into an ordered structure with hexagonal packing, which prevents the particles from further motion. Thus, there is a *spontaneous pinning effect as a result of particle ordering*.

Figure 4 shows the temporal change in the peak wave numbers (k_{max}) of the structure factor $S(k)$ (k is the wave number) for the OCL/OS (3/7) mixtures containing mobile glass particles [the same mixtures seen in Figs. 3(a)–3(c)]. The structure factor $S(k)$ is calculated from the 2D power spectrum of the original image [8]. The coarsening behavior can be approximated by the following power laws: For $\rho_n = 0.8 \times 10^6 \text{ cm}^{-2}$, $k_{\text{max}} \sim t^{-0.16}$; for $\rho_n = 1.3 \times 10^6 \text{ cm}^{-2}$, $k_{\text{max}} \sim t^{-1/3}$; and for $\rho_n = 4.7 \times 10^6 \text{ cm}^{-2}$, $k_{\text{max}} \sim t^{-0.11}$. The coarsening rate is fastest for $\rho_n = 1.3 \times 10^6 \text{ cm}^{-2}$. This is likely due to the interconnected structure and the absence of the strong pinning effect.

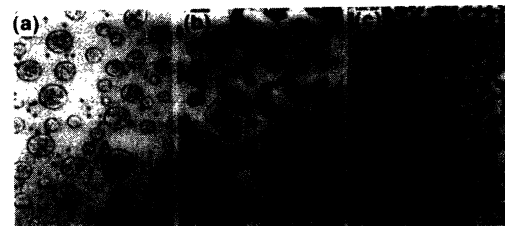


FIG. 3. Pattern evolution in OCL/OS (3/7) containing mobile glass particles at 60°C. The phase separation time is 1200 s for all. (a) $\rho_n = 0.8 \times 10^6 \text{ cm}^{-2}$, (b) $\rho_n = 1.3 \times 10^6 \text{ cm}^{-2}$, and (c) $\rho_n = 4.7 \times 10^6 \text{ cm}^{-2}$. The bar corresponds to 100 μm .

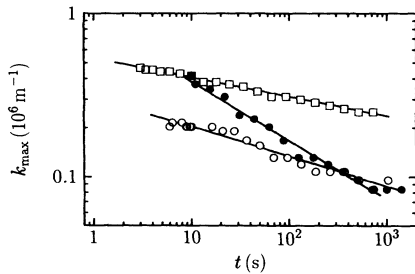


FIG. 4. Temporal change in the peak wave numbers (k_{\max}) of the power spectrum $S(k)$ for OCL/OS (3/7) containing mobile glass particles at 60°C. \circ : $\rho_n = 0.8 \times 10^6 \text{ cm}^{-2}$ [see Fig. 3(a)]; \bullet : $\rho_n = 1.3 \times 10^6 \text{ cm}^{-2}$ [see Fig. 3(b)]; and \square : $\rho_n = 4.7 \times 10^6 \text{ cm}^{-2}$ [see Fig. 3(c)].

It is also found that for the OS/OCL (5/5) mixture containing both glass particles (GP1) and spacers (GP2), the phase favoring glass particles form a matrix and the complementary phase forms droplets. During phase separation glass particles are included into the OCL-rich phase selectively.

First we discuss the static, energetic aspect of the problem. The total free energy of the system per unit volume can be given by

$$F = 4\pi a^2[\gamma_\alpha n_\alpha + \gamma_\beta n_\beta] + \frac{1}{d} \left[\gamma_\alpha \left(\Phi_\alpha + \frac{4}{3}\pi a^3 n_\alpha \right) + \gamma_\beta \left(\Phi_\beta + \frac{4}{3}\pi a^3 n_\beta \right) \right] + \sigma f(d).$$

Here the α and β phases are the OCL-rich and OS-rich phases, respectively, and n_α and n_β are the number of particles per unit volume in the α and β phases, respectively. Φ_α and Φ_β are the volume fractions of α and β phases vs the total volume of the sample including spheres, respectively, and thus $\Phi_\alpha + \Phi_\beta + \Phi_{\text{GP}} = 1$. a is the radius of the glass spheres. γ_α and γ_β are the interaction energy between the glass and the α and β phases, respectively. σ is the interfacial tension between the α and β phases. $f(d)$ is the total interfacial area between the α and β phases per unit volume. The first two terms in the above free energy are related to the wettability of the glass particles, the next two terms to the wettability of the glass plates, and the last term to the interfacial energy between the α and β phases. Here it should be noted that the wettability of the glass plates likely plays few roles in the late-stage phase separation after the bridge formation. The late-stage behavior between the plates is thus expected to be similar to that in bulk.

First we consider the effect of particle mobility on the pattern evolution under the influence of wetting. After the formation of a sharp interface, the wetting layers are quickly formed on the surfaces of both glass spheres and glass plates by the hydrodynamic process unique to nearly symmetric binary mixtures [4]. This wetting layer likely forms an interconnected structure so that the par-

ticles are essentially bridged by it. Once the droplets are bridged by the more wettable phase, the strong attractive interaction originating from the α - β interfacial energy acts between the droplets. This interaction is likely very long range because of the interconnected nature of the wetting layer. Thus, there are in essence no isolated particles. When this attractive force is weaker than the particle trapping force, particles cannot move (as seen in Fig. 1), and vice versa (as seen in Figs. 2 and 3). We now consider the pattern evolution in immobile and mobile cases. When the droplets are immobile (for $d = 2a$), the final structure is determined by the competition between $\Delta\gamma (= \gamma_\beta - \gamma_\alpha)$ and σ . For immobile glass particles, inclusion of the particle in the α phase opposes the formation of large domains. This likely leads to the final pattern composed of small domains where most of the particles are included in the α phase, even though there is a long boundary between the α and β phases. In addition to the energetic argument, consideration of the dynamics leads to the same conclusion. Coarsening of the droplet pattern is usually dominated by the evaporation-condensation and Brownian-coagulation mechanisms [1,9]. In our case, however, neither of these mechanisms should be applicable. Droplet motion is prevented by the pinning effect of the fixed glass spheres (*a strong spatial pinning effect*) and thus the Brownian-coagulation mechanism does not apply after formation of the metastable structure. Further, the local curvature of the droplet is not correlated with the droplet size and determined by the spatial distribution of the glass particles; thus the evaporation-condensation mechanism does not apply either. These considerations lead to the conclusion that after the bridging of glass particles by wetting from a growing α -phase droplet, the droplet pattern is stabilized for both static and kinetic reasons.

For the case of $d > 2a$, the glass spheres can move because there is no restriction on motion parallel to the glass plates. The system tries to reduce the free energy by lowering the energetic factors relating to $\Delta\gamma$ and σ . The former causes inclusion of the glass particles into the α -phase domains, while the latter causes coarsening of the domains. The pattern evolution can then be classified into the following three cases: (1) $\Phi_\alpha \gg \Phi_{\text{GP}}$, (2) $\Phi_\alpha \sim \Phi_{\text{GP}}$, and (3) $\Phi_\alpha \ll \Phi_{\text{GP}}$.

In case (1), the inclusion of the particles occurs first, and then the domains gradually grow by the wetting-layer-induced interaction as well as by the Brownian-coagulation and evaporation-condensation mechanisms. In contrast to the case of $d = 2a$, the glass particles are completely included inside the α -phase droplet because of their mobility. Thus the curvature is directly determined by the droplet size. As shown in Fig. 4, however, the coarsening rate is slow compared to the case without particles, where domains coarsen as $R \sim t^{1/3}$ (R is the characteristic domain size) [10]. The glass particles could reduce the translational motion of the droplet since the local-velocity difference between the fluid inside a droplet

and the spheres probably causes the additional friction to the droplet motion (*a weak spatial pinning effect of particles*). However, it is not clear whether this effect alone can lead to such a drastic reduction of the growth exponent or not, and thus further studies are highly desirable. For case (2), the packing density of the glass particles inside the α phase becomes very high and the glass particles form an ordered structure because of their geometrical confinement, which is a result of minimization of the $\Delta\gamma$ interaction. The ordered structure prevents the domains from deforming and coarsening further since there is a high potential barrier to deform the ordered hexagonal packing of the glass spheres. This spontaneous pinning effect due to particle ordering (*a shape-pinning effect of ordered particles*) slows down the coarsening of domains (see Fig. 4). Between cases (1) and (2), the coarsening rate becomes maximal ($R \sim t^{1/3}$) as shown in Fig. 4, because (i) as will be discussed below, the phase-separated structure becomes bicontinuous where the interfacial tension becomes important and leads to a quick hydrodynamic coarsening [9], and (ii) the particle density is not sufficiently high to induce a strong shape-pinning effect and domains can easily deform to reduce the interfacial area. For case (3), there is coexistence of the pinned pattern of closely packed glass spheres with those that cannot be included into the α phase.

Finally, we discuss the effect of the volume fraction of the glass particles on the final morphology. Since most of the glass particles are included in the α phase except for the case $\Phi_{GP} \gg \Phi_\alpha$, the apparent volume fraction of the α phase becomes $\Phi_\alpha + \Phi_{GP}$. Thus the bicontinuous structure appears when $\Phi_\alpha + \Phi_{GP} \sim 1/2$. The morphology can be changed by controlling Φ_{GP} , even for a fixed ratio between the α and β phases. Such behavior is actually observed in Fig. 3.

In summary, we found that the pattern evolution in an unstable binary liquid mixture containing glass particles is dominated by the dynamic interplay between phase separation and wetting. The mobility of the particles significantly affects both the coarsening dynamics and the final morphology. We showed that *spatial and shape-pinning effects of particles* significantly modify the coarsening dynamics of domains. The apparent symmetry of the order parameter can be changed by the volume fraction of the glass particles. The selective inclusion of solid particles into the more wettable phase and the resulting particle ordering are likely universal in any binary liquid mixtures including solid particles, irrespective of experimental settings such as particle shape, particle size, their distribution, and film thickness. Further, there is a possibility that a rodlike or disklike shape of the particle leads to the orientational ordering of the particles. Our system is likely one of the simplest and most ideal systems to study the effect of solid particles on phase separation in binary liquid mixtures. The interplay between phase

separation and wetting for mobile solid particles is a new problem, for which further experimental and theoretical studies are highly desirable. The present study is limited to semimacroscopic particles, but the basic idea is likely applicable to microscopic systems such as colloidal [6] if we include the effects of van der Waals and other relevant interactions, as well as the effect of thermal noise.

From an applications viewpoint, this study strongly indicates possibilities for control of the final domain size in phase separation by the spatial arrangement of a fixed solid phase, and also for control of a final morphology by the self-induced pinning effect through addition of a certain amount of mobile solid particles. These ideas could be applied to the physical design of composite materials including polymer alloys and polymer-dispersed liquid-crystal displays. By changing the volume fraction of particles, we can control the apparent symmetry of the composition, namely, whether the final pattern becomes bicontinuous or isolated. So far the structures of these mixtures have been considered from the static, energetic standpoint, but the present study also indicates the importance of the dynamic aspect.

One author (H.T.) is greatly indebted to AT&T Bell Laboratories, where most of this work was done, for the opportunity of a summer stay there. We express our thanks to Ube Nitto Chemicals Co. for kind provision of monodisperse glass spheres.

-
- [1] J.D. Gunton *et al.*, in *Phase Transition and Critical Phenomena*, edited by C. Domb and J.H. Lebowitz (Academic, London, 1983), Vol. 8.
 - [2] J.W. Cahn, *J. Chem. Phys.* **66**, 3667 (1977); D. Jasnow, *Rep. Prog. Phys.* **47**, 1059 (1984); P.G. de Gennes, *Rev. Mod. Phys.* **57**, 827 (1985).
 - [3] K. Williams and R.A. Dawe, *J. Colloid Interface Sci.* **117**, 81 (1987); A.J. Liu *et al.*, *Phys. Rev. Lett.* **65**, 1897 (1990); P. Guenoun *et al.*, *Phys. Rev. Lett.* **65**, 2406 (1990); R.A.L. Jones *et al.*, *Phys. Rev. Lett.* **66**, 1326 (1991); P. Wiltzius and A. Cumming, *Phys. Rev. Lett.* **66**, 3000 (1991); F. Bruder and R. Brenn, *Phys. Rev. Lett.* **69**, 624 (1992); J. Bodensohn and W.I. Goldberg, *Phys. Rev. A* **46**, 5084 (1992).
 - [4] H. Tanaka, *Phys. Rev. Lett.* **70**, 53 (1993); **70**, 2770 (1993); *Europhys. Lett.* **24**, 665 (1993).
 - [5] B.J. Frisken *et al.*, *Phys. Rev. Lett.* **66**, 2754 (1991), and references therein.
 - [6] D. Beysens and D. Esteve, *Phys. Rev. Lett.* **54**, 2123 (1985); V. Gurfein *et al.*, *Phys. Rev. A* **40**, 2543 (1989); P.D. Gallagher and J.V. Maher, *Phys. Rev. A* **46**, 2012 (1992).
 - [7] The essential feature is likely not affected by the way of experimental settings.
 - [8] H. Tanaka *et al.*, *J. Appl. Phys.* **59**, 3627 (1986); **65**, 4480 (1989).
 - [9] E.D. Siggia, *Phys. Rev. A* **20**, 595 (1979).
 - [10] H. Tanaka *et al.*, *Phys. Rev. Lett.* **65**, 3136 (1990).

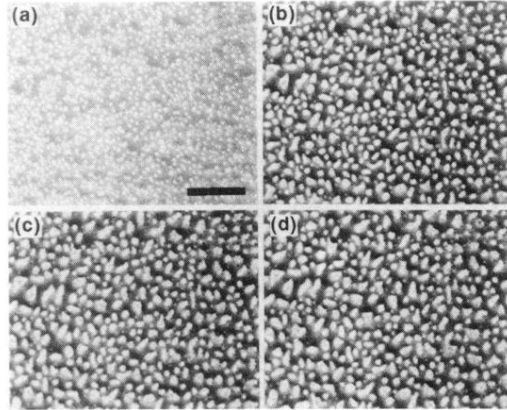


FIG. 1. Pattern evolution in OCL/OS (3/7) containing fixed glass particles at 100°C . (a) 25 s, (b) 60 s, (c) 240 s, and (d) 720 s after the quench. The bar corresponds to $100\ \mu\text{m}$.

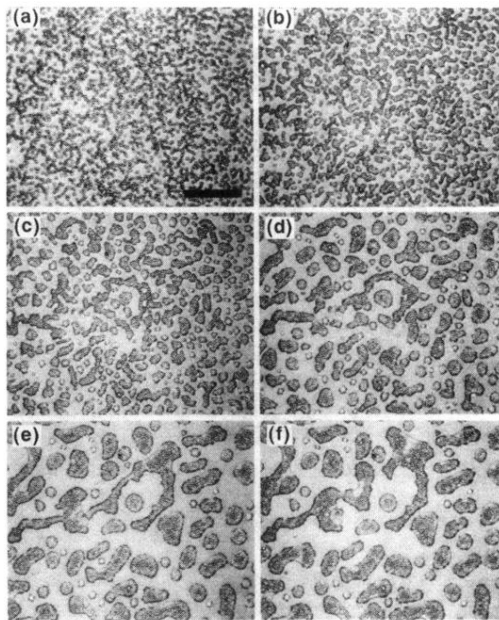


FIG. 2. Pattern evolution in OCL/OS (3/7) containing mobile glass particles at 100 °C. (a) 1 s, (b) 2 s, (c) 4 s, (d) 10 s, (e) 110 s, and (f) 950 s after the quench. The bar corresponds to 100 μm .

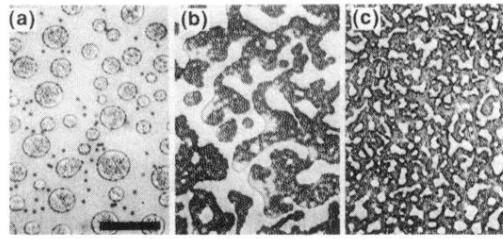


FIG. 3. Pattern evolution in OCL/OS (3/7) containing mobile glass particles at 60°C. The phase separation time is 1200 s for all. (a) $\rho_n = 0.8 \times 10^6 \text{ cm}^{-2}$, (b) $\rho_n = 1.3 \times 10^6 \text{ cm}^{-2}$, and (c) $\rho_n = 4.7 \times 10^6 \text{ cm}^{-2}$. The bar corresponds to 100 μm .